clean technologies

Article

Valorization of Biomass and Industrial Wastes as Alternative Fuels for Sustainable Cement Production

Ofelia Rivera Sasso [1], Caleb Carreño Gallardo [1,*], David Martin Soto Castillo [2], Omar Farid Ojeda Farias [2], Martin Bojorquez Carrillo [2], Carolina Prieto Gomez [2] and Jose Martin Herrera Ramirez [1,2,*]

[1] Centro de Investigacion en Materiales Avanzados, S.C. (CIMAV), Av. Miguel de Cervantes #120, Complejo Industrial Chihuahua, Chihuahua 31136, Mexico; ofelia.rivera@cimav.edu.mx
[2] GCC, Gerencia de Investigacion y Desarrollo, Vicente Suarez y Sexta S/N, Zona Industrial Nombre de Dios, Chihuahua 31105, Mexico; dsotoc@gcc.com (D.M.S.C.); ofojeda@gcc.com (O.F.O.F.); mbojorquezc@gcc.com (M.B.C.); cprietog@gcc.com (C.P.G.)
* Correspondence: caleb.carreno@cimav.edu.mx (C.C.G.); martin.herrera@cimav.edu.mx or jherreram@gcc.com (J.M.H.R.)

Abstract: The cement industry contributes around 7% of global anthropogenic carbon dioxide emissions, mainly from the combustion of fuels and limestone decomposition during clinker production. Using alternative fuels derived from wastes is a key strategy to reduce these emissions. However, alternative fuels vary in composition and heating value, so selecting appropriate ones is crucial to maintain clinker quality and manufacturing processes while minimizing environmental impact. This study evaluated various biomass and industrial wastes as potential alternative fuels, characterizing them based on proximate analysis, elemental and oxide composition, lower heating value, and bulk density. Sawdust, pecan nutshell, industrial hose waste, and plastic waste emerged as viable options as they met the suggested thresholds for heating value, chloride, moisture, and ash content. Industrial hose waste and plastic waste were most favorable with the highest heating values while meeting all the criteria. Conversely, wind blade waste, tire-derived fuel, and automotive shredder residue did not meet all the recommended criteria. Therefore, blending them with alternative and fossil fuels is necessary to preserve clinker quality and facilitate combustion. The findings of this research will serve as the basis for developing a computational model to optimize the blending of alternative fuels with fossil fuels for cement production.

Keywords: waste valorization; alternative fuels; carbon emissions; clinker production

Citation: Rivera Sasso, O.; Carreño Gallardo, C.; Soto Castillo, D.M.; Ojeda Farias, O.F.; Bojorquez Carrillo, M.; Prieto Gomez, C.; Herrera Ramirez, J.M. Valorization of Biomass and Industrial Wastes as Alternative Fuels for Sustainable Cement Production. *Clean Technol.* **2024**, *6*, 814–825. https://doi.org/10.3390/cleantechnol6020042

Academic Editor: Patricia Luis Alconero

Received: 9 May 2024
Revised: 5 June 2024
Accepted: 6 June 2024
Published: 14 June 2024

1. Introduction

The growth of urban populations has led to a surge in the construction of new residential buildings, driving a high demand for construction materials worldwide. Concrete is the most widely used construction material, followed only by water as the second most consumed material globally [1]. Consequently, this exerts an ecological impact, since the production of cement contributes to approximately 7% of global anthropogenic carbon dioxide emissions [2]. To foster more sustainable practices in cement production, several strategies have been implemented, including the following: (1) thermal substitution rate, (2) gas emission reduction, (3) energy efficiency, and (4) reduction in fossil fuels and increased use of alternative fuels, among others strategies [3–5].

Several key parameters are used to evaluate sustainability performance in the cement industry [6–8]. For instance, the effectiveness of alternative fuels is assessed by indicators such as the substitution rate of alternative fuel and biomass and the specific heat consumption for clinker production using alternative fuels, among others [8]. Therefore, to measure gas emissions, these can be evaluated as specific or absolute gas emissions [7]. The increased use of alternative fuels, while reducing reliance on fossil fuels, has the potential to reduce CO_2 emissions by up to 12%. Alternative fuels are expected to cover 22% and 43% of global cement kiln energy by 2030 and 2050, respectively [3].

On the other hand, global municipal solid waste generation is currently at 2.01 billion tons annually, and it is expected to grow up to 3.40 billion tons by 2050 [9]. Coprocessing wastes as alternative fuels and their partial substitution for fossil fuels in cement kilns offers a sustainable solution for managing and disposing wastes that cannot be reduced, reused, or recycled [10]. Furthermore, the high temperatures and long residence time, typical of cement kilns, can suppress the formation of undesirable compounds such as dioxins and furans during the combustion process [11].

Currently, the main alternative fuels used in the cement industry are residual oils and solvents, biomass, used tires and rubber waste, plastic waste, the thermal fraction of domestic waste, and sewage sludge [12]. Therefore, prior to their implementation, it is crucial to evaluate their potential impact on clinker quality, cement manufacturing processes, and environmental effects. Parameters such as (1) heating value; (2) alkali, sulfur, chloride, and metal content; (3) moisture and ash content; and (4) potential impact on operation stability should be considered.

Several research studies have been carried out on the potential use of biomass and industrial wastes as alternative fuels in the cement industry. These investigations have focused on modeling, life cycle analysis, and impact of integrating some wastes into cement production processes [12–14]. In 2019, Hashem et al. [15] explored the potential use of rubber and plastic wastes as alternative fuels in the cement industry. They characterized these wastes using various techniques and blended their ash residues with cement. Rubber waste exhibited higher contents of carbon, hydrogen, nitrogen, sulfur, and chlorine compared to plastic waste, indicating the likelihood of increased carbon and sulfur oxide emissions when using this waste as an alternative fuel. Incorporating these solid ash residues into cement blends at 5% and 10% resulted in reduced setting times, enhanced compressive strength, and accelerated hydration reactions. In 2021, Karpan et al. [16] conducted a study on the development of refuse-derived fuel (RDF) with a high heating value using mixed hazardous wastes and biomass, including rubber waste as hazardous waste and sawdust as biomass, among others. They characterized the RDF and found that substituting 15% of the coal did not result in any processing or quality issues in the cement production process. Additionally, this substitution led to reduced operational costs and diminished CO_2 emissions.

While certain wastes are not typically employed as alternative fuels, their substantial generation, such as wind blade waste and automotive shredder residue (ASR), has raised significant concern. Projections suggest that wind blade waste alone could reach 2.9 million tons by 2050 [17]. In efforts to mitigate this waste, research has explored its potential suitability as a material in mortar applications. Additionally, investigations have been conducted to assess its performance within a circular economy framework and to analyze its carbon footprint [18,19]. ASR is a mixture of several types of plastics, rubbers, foams, and other materials, and it constitutes approximately 30–35% of a vehicle after the metal recovery of end-of-life vehicles (ELVs). It is estimated that ELVs generate approximately 50 million tons of waste annually [20]. The ASR has been studied for both its inorganic components, which act as aggregates, and the combustion of its organic components [21,22]. However, neither wind blades waste nor automotive shredder residue have been studied as alternative fuels in the cement industry. Although several studies have explored using different wastes as alternative fuels, the factors influencing clinker production and environmental impacts remain unclear. A thorough, multidisciplinary investigation is needed to address these significant knowledge gaps and inform sustainable practices in this field.

Hence, the objective of this study was to assess the potential use of various biomass and industrial waste materials as alternative fuels in the cement industry to reduce carbon emissions and facilitate waste valorization. The physical and chemical properties of the wastes were characterized to evaluate their impact on both clinker quality and environmental factors. The wastes analyzed encompassed a variety of materials, including sawdust, pecan nutshell, wind blade waste, industrial hose waste, tire-derived fuel, plastic waste, and automotive shredder residue. These materials originate from various local industries located in the Central Corridor of North America, which covers Chihuahua State (Mexico) and the United States that consistently produce these types of waste streams. Bituminous coal, widely used as a fossil fuel in cement manufacturing, was also analyzed as a reference for comparison

2. Materials and Methods

2.1. Materials

The biomass and industrial wastes were collected from various local industries in the state of Chihuahua, Mexico. Table 1 shows the description of each sample and its identification. Each component of wind blade waste (WBW) was quantified individually to determine its respective weight percentage as follows: WBW-GF (77.3%), WBW-RS (4.7%), and WBW-SD (18.0%).

Table 1. Description and identification of samples.

Sample	Description	Identification
Sawdust	Irregularly shaped wood shavings	SD
Pecan nutshell	Irregularly shaped crushed pecan nutshell	PNS
Wind blade waste	Pieces of wind blade exhibiting varying proportions of glass fiber (WBW-GF), resin (WBW-RS), and sawdust (WBW-SD)	WBW
Industrial hose waste	Pieces consisting of a mixture of various types of hoses	IHW
Tire-derived fuel	Irregularly shaped tire parts	TDF
Plastic waste	Pieces composed of a blend of rubber (PW-RB), polyurethane (PW-PL), resin (PW-RS), car dashboard (PW-CD), and fabrics (PW-FB) combined in balanced proportions	PW
Automotive shredder residue	Irregularly shaped plastic and metal parts	ASR

2.2. Sample Preparation

The preparation of samples for characterization varied due to their different nature. WBW, IHW, PW, and ASR samples were crushed to reduce their size to 1 cm using a Dewalt table jigsaw (Dewalt, Ciudad Juarez, Mexico). Subsequently, each waste was ground to 0.5 mm mesh in a Retsch SM 100 cutting mill (Retsch, Newtown, PA, USA), followed by drying and preservation in a desiccator. For characterizing the waste ashes, each waste was calcined for 1 h at the temperature where its mass loss, determined through thermogravimetric analysis, became constant.

2.3. Test Methods

The proximate analysis of samples was conducted using a TA Instruments SDT Q600 thermogravimetric analyzer (TA Instruments, New Castle, DE, USA) according to the ASTM D7582 standard [23]. The carbon, hydrogen, oxygen, sulfur, and nitrogen contents were determined with a Thermo Fisher Scientific FlashSmart elemental analyzer (Thermo Fisher Scientific, Waltham, MA, USA). Total chloride analysis was conducted using the oxygen vessel combustion/ion selective electrode method in accordance with the ASTM D4208 standard [24]. The lower heating value (LHV) was determined on dry basis samples using a LECO AC500 isoperibol calorimeter (LECO, Monterrey, Mexico) according to the ASTM D5865/D5865M standard [25]. The bulk density was evaluated according to the ASTM E873 and ASTM D291/D291M standards [26,27].

To identify the functional groups of samples, Fourier transform infrared spectroscopy (FTIR) was performed using a Shimadzu IRAffinity-1S FTIR spectrometer (Shimadzu, Carlsbad, CA, USA) in the attenuated total reflectance mode. The spectra were recorded in the range of 4000–450 cm^{-1} with a resolution of 4 cm^{-1} and 30 successive scans.

The chemical composition of the sample ashes was analyzed by X-ray fluorescence (XRF) using an Epsilon 3XLE spectrometer (Malvern Panalytical, Westborough, MA, USA) at 20 kV and 10 mA. The crystalline phases of sample ashes were evaluated by X-ray diffraction (XRD) using an X'Pert PRO MPD diffractometer (Malvern Panalytical, Westborough, MA, USA) coupled to a PW3011/20X' accelerator detector using the Bragg–Brentano geometry at 40 kV and 15 mA.

3. Results and Discussion

The proximate, elemental, and physical analysis results are shown in Table 2. The moisture content of the wastes is below the recommended threshold of 10.0% [28] and lower than that of coal, except for SD and PNS. It is important to note that a higher moisture content would result in the diversion of heat from the combustion of the fuel during the calcination of the raw meal. The wastes have a higher volatile content compared to coal, suggesting that they would reach their ignition temperature sooner and combust faster than coal [29]. The fixed carbon content of all the wastes is lower than that of coal. However, some wastes exhibit a relatively elevated fixed carbon content, such as IHW and TDF, leading to generally higher heating values and extended combustion times. This is attributed to the increased carbon density, resulting in a more efficient combustion process [30]. The ash content of most of the wastes and coal is below the recommended limit of 12.0% [31], except for WBW and ASR. The ashes from fuel absorb heat, and a lower ash content would result in better heat transfer inside the kiln [32]. Moreover, the ashes from the wastes will be incorporated with the raw meal during calcination, which may affect the quality of the clinker.

Table 2. Proximate, elemental, and physical analysis of wastes and bituminous coal.

	SD	PNS	WBW	IHW	TDF	PW	ASR	Coal
Proximate analysis (wt%)								
Moisture	5.2	4.1	2.0	0.4	0.7	0.2	1.2	3.0
Volatile matter	86.7	72.5	38.9	73.2	67.2	89.4	59.5	41.5
Fixed carbon	7.4	19.0	4.1	21.2	27.5	9.4	18.6	45.8
Ash	0.7	4.4	55.0	5.2	4.9	1.0	20.7	10.7
Elemental analysis on dry basis (wt%)								
C	45.50	50.80	31.30	82.86	90.0	77.40	49.10	84.26
H	5.80	5.90	3.51	5.23	7.98	8.10	5.90	3.27
O	40.50	32.76	10.95	7.58	1.06	13.26	17.86	9.83
N	-	-	1.26	2.70	0.34	1.17	1.08	2.64
S	0.03	0.03	-	-	0.14	-	-	0.83
Cl^-	0.01	-	1.11	0.03	0.17	0.05	0.15	0.04
Physical analysis								
LHV (MJ/kg)	16.9	18.0	11.5	34.0	36.5	29.0	22.0	27.8
Bulk density (g/cm^3)	0.29	0.82	0.40	0.37	0.39	0.20	0.44	0.62

Overall, most wastes have a lower carbon content than coal, except for TDF. However, all wastes exhibit a higher hydrogen content than coal, and most of them show elevated oxygen content compared to coal, except for IHW and TDF. A fuel with high carbon and hydrogen contents releases more energy during combustion, corresponding to its heating value. Conversely, a high oxygen content negatively impacts the heating value of the fuel [33]. The nitrogen content of most wastes, except for IHW, and the sulfur content of all wastes are lower than those of coal. It is noteworthy that the carbon, nitrogen, and sulfur contents of both wastes and coal can serve as indicators for predicting potential emissions of gases, such as CO_x, NO_x, and SO_2. In this regard, wastes can be predicted to emit less combustion gases than coal. The chloride content in the wastes is below the recommended threshold of 0.2% [34], except for WBW. Chloride affects cement durability by solubilizing calcium. At high concentrations, chloride may also destabilize portlandite, leading to the formation of detrimental calcium chlorohydroxy hydrates [35]. Moreover, chloride can react with alkali metals to form crusts and blockages in the kiln and preheater [36].

The LHV of the wastes surpasses the recommended value of 14 MJ/kg to be considered as alternative fuels [34], except for WBW. The LHV of IHW, TDF, and PW exceeds that of coal, indicating higher energy release during clinker calcination, which is beneficial as a fuel. The bulk density of the wastes is lower than that of coal, except for PNS. A reduced bulk density can hinder fuel feeding into the kiln as the fuel may be more prone to expulsion from the kiln [37].

The proximate, elemental, and physical characterization results obtained for SD in this study align closely with the findings reported by Varma and Mondal [38]. Likewise, these analyses for PNS reveal similarities with the results of Aldana et al. for pecan nut shells, walnut shells, and hazelnut shells [39]. For WBW, the proximate and elemental results fall within the ranges of the basic components of wind turbine blades [40], while no information was found for the physical analysis. The findings from the proximate, elemental, and physical analysis of IHW exhibit similarities with those of rubber. However, it is noteworthy that the LHV of the rubber in this study exhibits a higher content compared to previous studies [12,41]. The results of the proximate, elemental, and physical analyses of TDF uncover similarities with those of waste tire studies [42,43]. Similarly, the results for automobile shredder residue (ASR) are comparable to those reported in other ASR studies [20,44,45]. For PW, the proximate, elemental, and physical analyses highlight similarities with previous studies; however, the volatile matter content was lower than the values reported in [12,46].

As depicted above, high contents of carbon (%C) and hydrogen (%H) contribute to a higher heating value [33]. However, %C is crucial in predicting the CO_2 released by the fuel. Thus, Figure 1 displays the %C/LHV ratio for the wastes, which is lower than coal. This suggests that wastes would emit less CO_2 per MJ/kg of heat when compared to coal. Among the wastes, ASR has the lowest %C/LHV ratio due to its lower carbon content and significant hydrogen contribution to its LHV. A more sustainable fuel should have a higher heating value and lower CO_2 emissions.

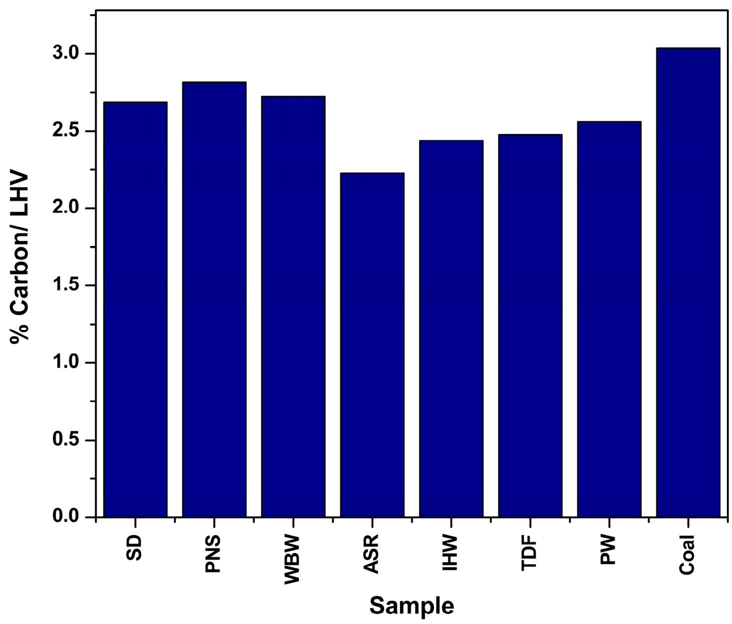

Figure 1. %C/LHV ratio of the wastes.

The FTIR results of biomass wastes (SD and PNS) and the WBW and PW components are presented in Figures 2–4, respectively; the FTIR bands and their corresponding assignments are summarized in Table 3. The SD spectrum (Figure 2) reveals signals in the range of 900 to 1250 cm^{-1}, indicating the presence of cellulose. The PNS spectrum (Figure 2) exhibits the signals mentioned above along with another signal at 1600 cm^{-1}, which are attributed to carboxymethyl cellulose [47]. The WBW-GF, WBW-RS, and WBW-SD spectra (Figure 3) reveal signals at 900–1250 cm^{-1}, 1060 cm^{-1}, 1500 cm^{-1}, 2800–3000 cm^{-1}, and 3400 cm^{-1}, which are attributed to epoxy resin and glass fiber [48,49]. However, in the range of 900 to 1250 cm^{-1}, there is a wide band that suggests the presence of cellulose [47]. For IHW, it was not possible to identify functional groups due to interference from carbon black. As for TDF, the functional groups of elastomeric polymers could not be identified due to interference from carbon black and other mineral components. The PW-RB spectrum (Figure 4) reveals signals at 1300–1500 cm^{-1} and 2800–3000 cm^{-1} assigned to polypropylene [50]. Additionally, there are signals at 700 cm^{-1}, corresponding to four consecutive CH_2 groups, and at 1450 cm^{-1}, which are attributed to polyethylene [51]. The PW-PL and PW-CD spectra display signals at 960 cm^{-1}, 1160 cm^{-1}, 1250 cm^{-1}, 1650–1750 cm^{-1}, 2800–3000 cm^{-1}, and 3300 cm^{-1}, all of them from polyurethane [52]. The PW-RS spectrum exhibits signals at 1060–1274 cm^{-1}, 1010–1500 cm^{-1}, 1760 cm^{-1}, and 2800–3000 cm^{-1}, indicating the presence of polycarbonate [53]. The PW-FB spectrum exhibits signals at 717 cm^{-1}, 960–1330 cm^{-1}, 1700 cm^{-1}, and 2800–3000 cm^{-1}, which are ascribed to polyester [51].

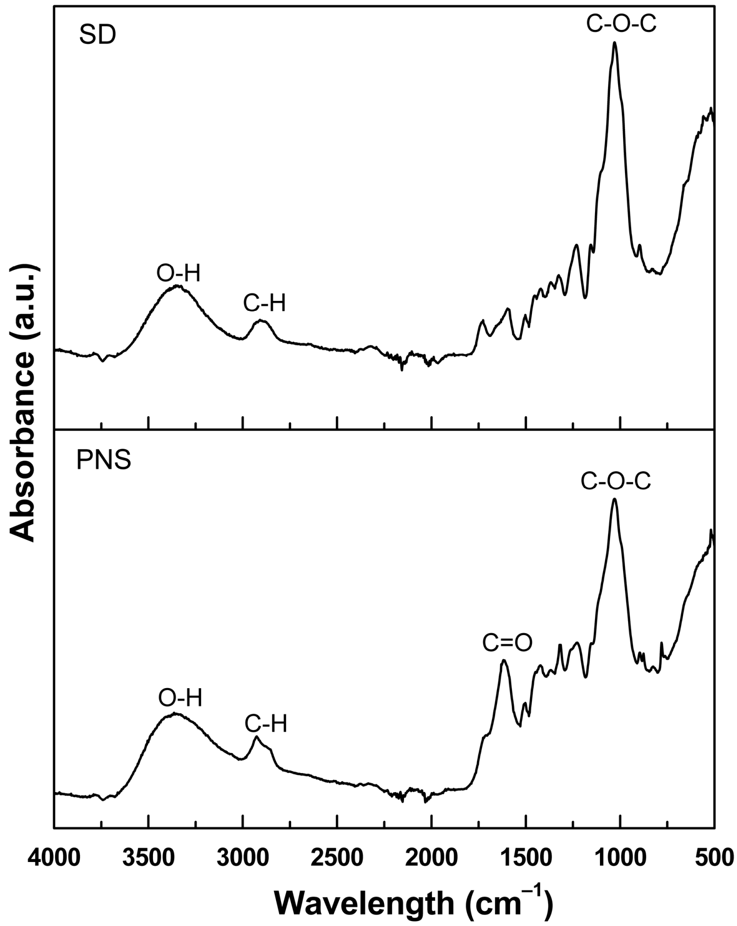

Figure 2. FTIR spectra of biomass wastes.

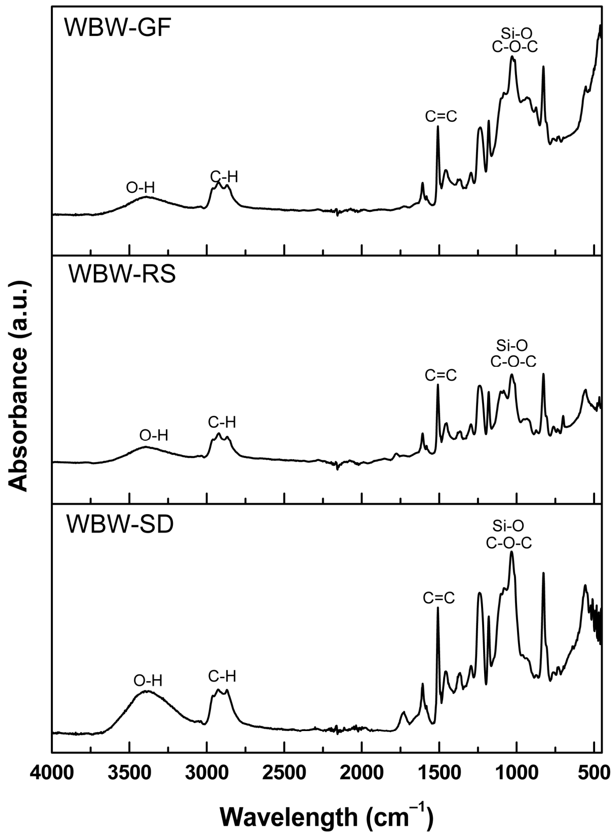

Figure 3. FTIR spectra of the WBW components.

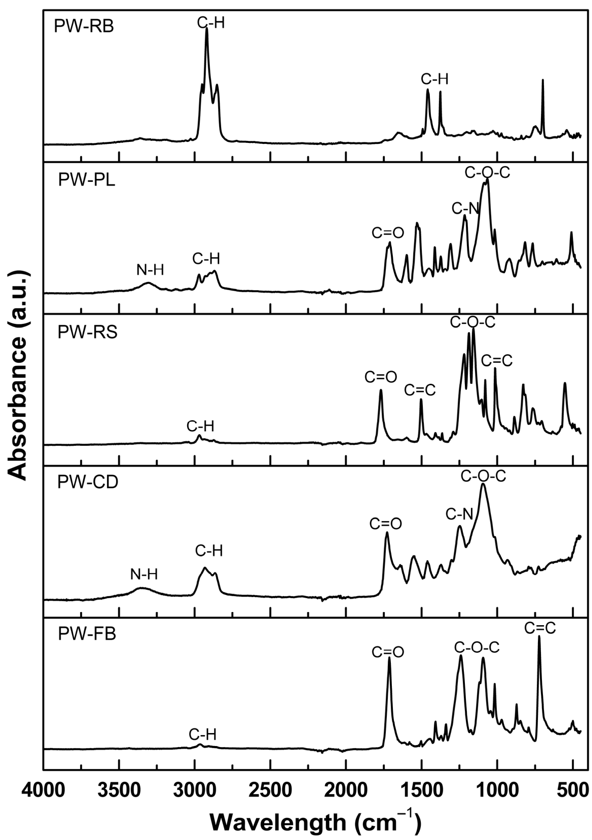

Figure 4. FTIR spectra of the PW components.

Table 3. Assignments of the FTIR bands.

Peak (cm^{-1})	Bond
720, 1010, 1500, 1600	C=C bending
960–1300	C-O-C stretching
1060	Si-O stretching
1250	C-N stretching
1370, 1450, 1550	C-H bending
1650–1750	C=O stretching
2800–3000	C-H stretching
3300	N-H stretching
3400	O-H stretching

The sample components identified by FTIR do not affect the quality of the clinker since most of them may volatize during the initial stage of combustion, as pointed out in the proximate analysis. Subsequently, they will oxidize at high temperatures, potentially influencing their kinetics. In the case of the WBW components, there are Si-O signals that could be corroborated by XRF analysis, indicating the presence of SiO_2, which remains in the ash residue. In the case of PW-PL and PW-CD, they have signals of N-H, which could lead to the formation of NO_x during the combustion.

Figure 5 shows the chemical composition of waste ashes. Most of them have a lower oxide compound content compared to coal, as evidenced by the ash percentage, except for WBW and ASR. The presence of SiO_2, Al_2O_3, Fe_2O_3, and CaO in the ashes of these wastes may influence the chemical composition of the clinker, affecting parameters such as the silica ratio, aluminum ratio, and lime saturation factor. Both of them show the highest levels of heavy metal oxides (ZnO and Cr_2O_3) among all the wastes, surpassing the recommended threshold of 0.25% [34]. ZnO influences cement by increasing the setting time and reducing its compressive strength [54,55]. Cr_2O_3 inhibits the formation of alite, which is one of the main phases of cement, thus reducing the setting time of cement [54,56]. The content of other oxide compounds was low enough to presumably have minimal impact on the clinker.

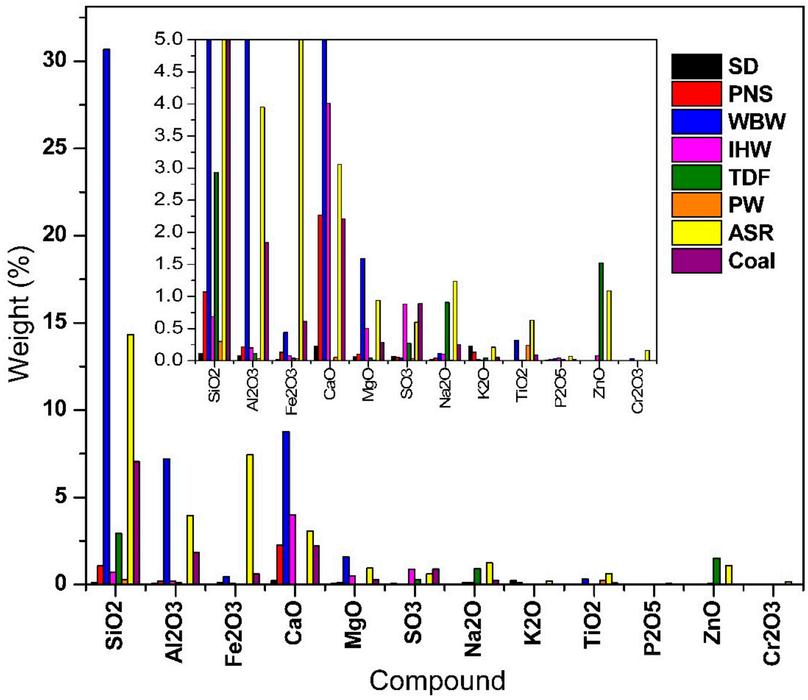

Figure 5. Results of XRF analysis of wastes and bituminous coal. The inset graph displays an enlarged view of the data up to 5 wt%.

Figure 6 shows the XRD patterns of the analyzed waste ashes. The main phases identified in the samples are as follows: calcium oxide (CaO), magnesium oxide (MgO), and potassium sulfate (K_2SO_4) for SD; calcium oxide (CaO) and potassium calcium magnesium sulfate ($K_2CaMg(SO_4)_3$) for PNS; calcium oxide silicate (Ca_3SiO_5), silicon oxide (SiO_2), and aluminum silicate (Al_2SiO_5) for WBW; calcium oxide (CaO), calcium sulfate ($CaSO_4$), silicon oxide (SiO_2), and magnesium oxide (MgO) for IHW; zinc silicate (Zn_2SiO_4) and zinc hydroxide ($Zn(OH)_2$) for TDF; titanium oxide (TiO_2), sodium titanium iron oxide ($NaTi_3FeO_8$), calcium titanium oxide ($CaTiO_3$), and silicon oxide (SiO_2) for PW; and silicon oxide (SiO_2), titanium oxide sulfate ($Ti(SO_4)O$), and magnesium iron oxide ($MgFe_2O_4$) for ASR. These crystalline phases are consistent with the oxide content found by XRF (Figure 5). The crystalline phases of SD, PNS, IHW, and PW may not significantly affect the clinker composition, owing to their low ash content (Table 2). On the contrary, the crystalline phases of WBW and ASR could affect the composition of the clinker due to its high ash content (Table 2). Regarding TDF, although its ash content is relatively low (Table 2), its Zn-based crystalline phases may have the potential to influence clinker quality.

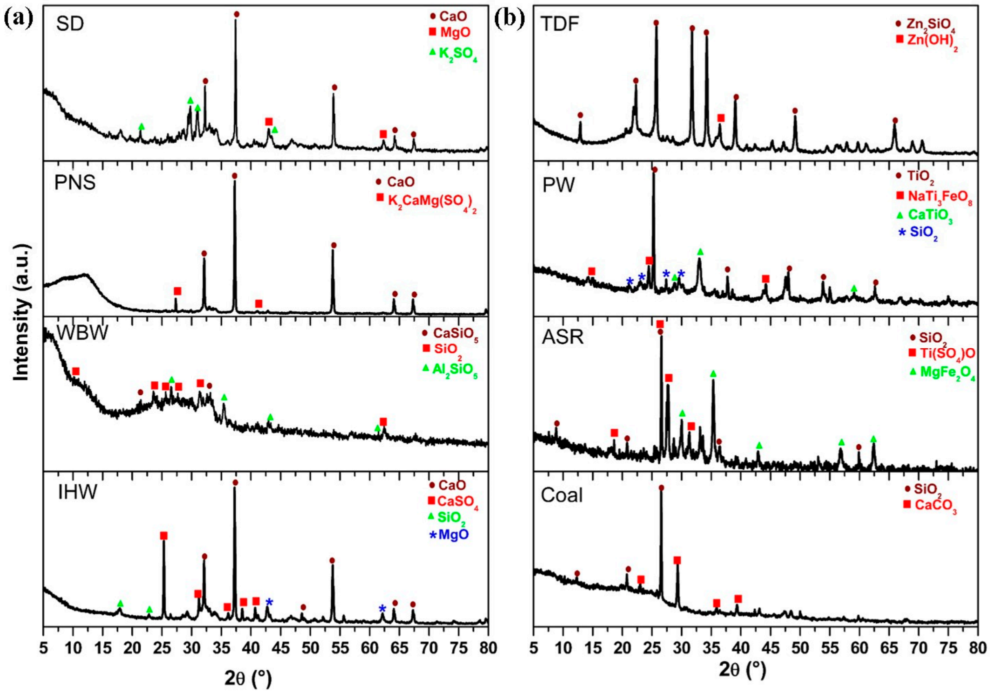

Figure 6. Crystalline phases of (**a**) SD, PNS, WBW, and IHW and (**b**) TDF, PW, ASR, and coal.

4. Conclusions

Based on the results of this study, the main conclusions are as follows:

(a) Sawdust, pecan nutshell, industrial hose waste, and plastic waste have been demonstrated as viable alternative fuels for partially substituting fossil fuels in cement kilns, as their properties, including heating value, moisture, ash, heavy metals, and chlorides content, align with the recommended specifications for alternative fuel sources.

(b) Among the samples evaluated, industrial hose waste and plastic waste are the most promising candidates for alternative fuels in cement kilns as they exhibit optimal characteristics that conform to all the recommended parameters. Notably, these two wastes have the highest calorific values and elevated carbon and hydrogen content, making them energetically dense and well suited to partially replace conventional fossil fuels while minimizing environmental impact.

(c) The substantial generation of certain uncommon wastes like wind blade waste and automotive shredder residue (ASR) has raised significant concerns about their disposal. However, these two wastes, together with tire-derived fuel, do not meet all the recommended criteria, making them less desirable as alternative fuels. Specifically, wind blade waste and automotive shredder residue exhibit an excessively high ash content, which can adversely impact the combustion process. In addition, the former does not reach the desired heating value threshold and exceeds the acceptable chloride content limit, further diminishing its suitability as an alternative fuel in cement kilns.

(d) Tire-derived fuel and automotive shredder residue exhibit elevated levels of heavy metals, surpassing the recommended thresholds for their utilization as alternative fuels.

(e) Consequently, to effectively exploit the potential of wind blade waste, tire-derived fuel, and automotive shredder residue as alternative fuels in cement kilns, a proper blending strategy would be necessary. This approach would involve the use of these wastes with other alternative fuels and fossil fuels in optimized proportions.

(f) The findings of this research will serve as the basis for developing a computational model, currently under progress, to optimize the blending of alternative fuels with fossil fuels for cement production. Optimal blending would not only help mitigate the adverse impacts of excessive ash, chlorides, and heavy metals but also ensure the maintenance of clinker quality and facilitate an efficient combustion process within the kiln system.

Author Contributions: Conceptualization, C.P.G. and J.M.H.R.; methodology, O.R.S., C.C.G., D.M.S.C. and M.B.C.; validation, C.C.G., M.B.C. and O.F.O.F.; formal analysis, O.F.O.F., D.M.S.C., M.B.C. and J.M.H.R.; investigation, O.R.S. and J.M.H.R.; resources, C.P.G.; writing—original draft preparation, O.R.S.; writing—review and editing, O.F.O.F., M.B.C., C.P.G. and J.M.H.R.; visualization, O.F.O.F. and J.M.H.R.; supervision, C.P.G. and J.M.H.R.; project administration, C.P.G. and J.M.H.R.; funding acquisition, J.M.H.R. All authors have read and agreed to the published version of the manuscript.

Funding: This research was funded by Convocatoria Interna para Proyectos de Investigacion y Desarrollo Tecnologico 2024 (CIMAV), grant number PI-2024-15.

Institutional Review Board Statement: Not applicable.

Informed Consent Statement: Not applicable.

Data Availability Statement: Data are contained within the article.

Acknowledgments: ORS thanks CONAHCYT for her scholarship (grant number 874347). Thanks are expressed to D. Lardizabal Gutierrez, J.E. Ledezma Sillas, L. de la Torre Saenz, M. Roman Aguirre, A.I. Gonzalez Jaquez, A. Benavides Montoya, F.G. Nevarez Vargas, L.A. Lozoya Marquez, O. Velazquez Meraz, V. Mancinas Vazquez, and all the GCC R&D team.

Conflicts of Interest: The authors declare that the research was conducted in the absence of any commercial or commercial or financial relationships that could be construed as a potential conflict of interest.

References

1. Makul, N. Advanced smart concrete—A review of current progress, benefits and challenges. *J. Clean. Prod.* **2020**, *274*, 122899. [CrossRef]
2. Concrete Future. *The GCCA 2050 Cement and Concrete Industry Roadmap for Net Zero Concrete*; Global Cement and Concrete Association (GCCA): London, UK, 2021.
3. *Global Cement and Concrete Industry Announces Roadmap to Achieve Groundbreaking 'Net Zero' CO_2 Emissions by 2050*; Global Cement and Concrete Association (GCCA): London, UK, 2021.
4. Cement Best Practices and Reporting. 2019. Available online: https://gccassociation.org/sustainability-innovation/cement-best-practices-and-reporting/ (accessed on 29 May 2024).
5. Cement Industry Net Zero Progress Report. 2023. Available online: https://gccassociation.org/cement-industry-net-zero-progress/ (accessed on 29 May 2024).
6. *GCCA Sustainability Framework Guidelines*; Global Cement and Concrete Association (GCCA): London, UK, 2022.
7. *GCCA Sustainability Guidelines for the Monitoring and Reporting of Emissions from Cement Manufacturing*; Global Cement and Concrete Association (GCCA): London, UK, 2019.
8. *GCCA Sustainability Guidelines for Co-Processing Fuels and Raw Materials in Cement Manufacturing*; Global Cement and Concrete Association (GCCA): London, UK, 2019.

9. Kaza, S.; Yao, L.; Bhada-Tata, P.; Van Woerden, F. *What a Waste 2.0: A Global Snapshot of Solid Waste Management to 2050*; World Bank Publications: Washington, DC, USA, 2018.
10. *GCCA Sustainability Guidelines for the Monitoring and Reporting of CO_2 Emissions from Cement Manufacturing*; Global Cement and Concrete Association (GCCA): London, UK, 2019.
11. Karstensen, K.H. Formation, release and control of dioxins in cement kilns. *Chemosphere* **2008**, *70*, 543–560. [CrossRef] [PubMed]
12. Zieri, W.; Ismail, I. Alternative fuels from waste products in cement industry. In *Handbook of Ecomaterials*; Springer Nature: Cham, Switzerland, 2018.
13. Rahman, A.; Rasul, M.G.; Khan, M.M.K.; Sharma, S.C. Assessment of energy performance and emission control using alternative fuels in cement industry through a process model. *Energies* **2017**, *10*, 1996. [CrossRef]
14. Chatterjee, A.; Sui, T. Alternative fuels–effects on clinker process and properties. *Cem. Concr. Res.* **2019**, *123*, 105777. [CrossRef]
15. Hashem, F.S.; Razek, T.A.; Mashout, H.A. Rubber and plastic wastes as alternative refused fuel in cement industry. *Constr. Build. Mater.* **2019**, *212*, 275–282. [CrossRef]
16. Karpan, B.; Raman, A.A.A.; Aroua, M.K.T. Waste-to-energy: Coal-like refuse derived fuel from hazardous waste and biomass mixture. *Process Saf. Environ. Prot.* **2021**, *149*, 655–664. [CrossRef]
17. Liu, P.; Barlow, C. Wind turbine blade waste in 2050. *Waste Manag.* **2017**, *62*, 229–240. [CrossRef]
18. Oliveira, P.S.; Antunes, M.L.P.; da Cruz, N.C.; Rangel, E.C.; de Azevedo, A.R.G.; Durrant, S.F. Use of waste collected from wind turbine blade production as an eco-friendly ingredient in mortars for civil construction. *J. Clean. Prod.* **2020**, *274*, 122948. [CrossRef]
19. Diez-Cañamero, B.; Mendoza, J.M.F. Circular economy performance and carbon footprint of wind turbine blade waste management alternatives. *Waste Manag.* **2023**, *164*, 94–105. [CrossRef] [PubMed]
20. Kohli, I.; Srivatsa, S.C.; Das, O.; Devasahayam, S.; Singh Raman, R.K.; Bhattacharya, S. Pyrolysis of Automotive Shredder Residue (ASR): Thermogravimetry, In-Situ Synchrotron IR and Gas-Phase IR of Polymeric Components. *Polymers* **2023**, *15*, 3650. [CrossRef]
21. Acha, E.; Lopez-Urionabarrenechea, A.; Delgado, C.; Martinez-Canibano, L.; Perez-Martinez, B.B.; Serras-Malillos, A.; Caballero, B.M.; Unamunzaga, L.; Dosal, E.; Montes, N.; et al. Combustion of a Solid Recovered Fuel (SRF) Produced from the Polymeric Fraction of Automotive Shredder Residue (ASR). *Polymers* **2021**, *13*, 3807. [CrossRef] [PubMed]
22. Colangelo, F.; Messina, F.; Di Palma, L.; Cioffi, R. Recycling of non-metallic automotive shredder residues and coal fly-ash in cold-bonded aggregates for sustainable concrete. *Compos. Part B Eng.* **2017**, *116*, 46–52. [CrossRef]
23. *ASTM D7582-15*; Standard Test Methods for Proximate Analysis of Coal and Coke by Macro Thermogravimetric Analysis. ASTM: West Conshohocken, PA, USA, 2015.
24. *ASTM D4208-19*; Standard Test Method for Total Chlorine in Coal by the Oxygen Vessel Combustion/Ion Selective Electrode Method. ASTM: West Conshohocken, PA, USA, 2019.
25. *ASTM D5865/D5865M-19*; Standard Test Method for Gross Calorific Value of Coal and Coke. ASTM: West Conshohocken, PA, USA, 2019.
26. *ASTM E873-82(2019)*; Standard Test Method for Bulk Density of Densified Particulate Biomass Fuels. ASTM: West Conshohocken, PA, USA, 2019.
27. *ASTM D291/D291M-20*; Standard Test Method for Bulk Density of Crushed Bituminous Coal. ASTM: West Conshohocken, PA, USA, 2020.
28. Alsop, P.A. *Cement Plant Operations Handbook: For Dry Process Plants*; Tradeship Publications Ltd.: Luxembourg, 2007.
29. Riaza, J.; Gibbins, J.; Chalmers, H. Ignition and combustion of single particles of coal and biomass. *Fuel* **2017**, *202*, 650–655. [CrossRef]
30. Arisanti, R.; Yusuf, M.; Faizal, M. Study of the effect of proximate, ultimate, and calorific value analysis on methane gas emission (CH4) on combustion of coal for sustainable environment. *Sci. Technol. Indones.* **2018**, *3*, 100–106. [CrossRef]
31. Equipment, C. Fuels in the Cement Industry. 5 May 2024. Available online: https://www.cementequipment.org/home/fuels-in-the-cement-industry/ (accessed on 5 May 2024).
32. Zbogar, A.; Frandsen, F.J.; Jensen, P.A.; Glarborg, P. Heat transfer in ash deposits: A modelling tool-box. *Prog. Energy Combust. Sci.* **2005**, *31*, 371–421. [CrossRef]
33. Demirbas, A. Effects of moisture and hydrogen content on the heating value of fuels. *Energy Sources Part A Recovery Util. Environ. Eff.* **2007**, *29*, 649–655. [CrossRef]
34. Rahman, A.; Rasul, M.G.; Khan, M.M.K.; Sharma, S. Impact of alternative fuels on the cement manufacturing plant performance: An overview. *Procedia Eng.* **2013**, *56*, 393–400. [CrossRef]
35. Galan, I.; Glasser, F.P. Chloride in cement. *Adv. Cem. Res.* **2015**, *27*, 63–97. [CrossRef]
36. Wang, Y.; Zhu, H.; Jiang, X.; Lv, G.; Yan, J. Study on the evolution and transformation of Cl during Co-incineration of a mixture of rectification residue and raw meal of a cement kiln. *Waste Manag.* **2019**, *84*, 112–118. [CrossRef]
37. Yu'nan, Z.; Jianzhong, L.; Liang, D.; Wei, S.; Weijuan, Y.; Junhu, Z. Effect of particle size and oxygen content on ignition and combustion of aluminum particles. *Chin. J. Aeronaut.* **2017**, *30*, 1835–1843.
38. Varma, A.K.; Mondal, P. Physicochemical characterization and pyrolysis kinetics of wood sawdust. *Energy Sources Part A: Recovery Util. Environ. Eff.* **2016**, *38*, 2536–2544. [CrossRef]
39. Aldana, H.; Lozano, F.J.; Acevedo, J.; Mendoza, A. Thermogravimetric characterization and gasification of pecan nut shells. *Bioresour. Technol.* **2015**, *198*, 634–641. [CrossRef] [PubMed]

40. Ge, L.; Xu, C.; Feng, H.; Jiang, H.; Li, X.; Lu, Y.; Sun, Z.; Wang, Y.; Xu, C. Study on isothermal pyrolysis and product characteristics of basic components of waste wind turbine blades. *J. Anal. Appl. Pyrolysis* **2023**, *171*, 105964. [CrossRef]
41. Geng, J.; Li, L.F.; Wang, W.L.; Chang, J.M.; Xia, C.L.; Cai, L.P.; Shi, S.Q. Fabrication of activated carbon using two-step co-pyrolysis of used rubber and larch sawdust. *BioResources* **2017**, *12*, 8641–8652. [CrossRef]
42. Erliyanti, N.K.; Sangian, H.F.; Susianto, S.; Altway, A. The preparation of fixed carbon derived from waste tyre using pyrolysis. *Sci. Study Res. Chem. Chem. Eng.* **2015**, *16*, 343–352.
43. Pan, D.L.; Jiang, W.T.; Guo, R.T.; Huang, Y.; Pan, W.G. Thermogravimetric and Kinetic Analysis of Co-Combustion of Waste Tires and Coal Blends. *ACS Omega* **2021**, *6*, 5479–5484. [CrossRef] [PubMed]
44. Vijayan, S.K.; Kibria, M.A.; Uddin, M.H.; Bhattacharya, S. Pretreatment of Automotive Shredder Residues, Their Chemical Characterisation, and Pyrolysis Kinetics. *Sustainability* **2021**, *13*, 10549. [CrossRef]
45. Harder, M.; Forton, O. A Critical Review of Developments in the Pyrolysis of Automotive Shredder Residue. *J. Anal. Appl. Pyrolysis* **2007**, *79*, 387–394. [CrossRef]
46. Dubdub, I.J.; Al-Yaari, M. Pyrolysis of Mixed Plastic Waste: I. Kinetic Study. *Materials* **2020**, *13*, 4912. [CrossRef]
47. Abderrahim, B.; Abderrahman, E.; Mohamed, A.; Fatima, T.; Abdesselam, T.; Krim, O. Kinetic thermal degradation of cellulose, polybutylene succinate and a green composite: Comparative study. *World J. Environ. Eng.* **2015**, *3*, 95–110.
48. Caban, R. FTIR-ATR spectroscopic, thermal and microstructural studies on polypropylene-glass fiber composites. *J. Mol. Struct.* **2022**, *1264*, 133181. [CrossRef]
49. Wu, Z.; Li, S.; Liu, M.; Wang, Z.; Liu, X. Liquid oxygen compatible epoxy resin: Modification and characterization. *RSC Adv.* **2015**, *5*, 11325–11333. [CrossRef]
50. Fang, J.; Zhang, L.; Sutton, D.; Wang, X.; Lin, T. Needleless melt-electrospinning of polypropylene nanofibres. *J. Nanomater.* **2012**, *2012*, 382639. [CrossRef]
51. Tariq, A.; Afzal, A.; Rashid, I.A.; Shakir, M.F. Study of thermal, morphological, barrier and viscoelastic properties of PP grafted with maleic anhydride (PP-g-MAH) and PET blends. *J. Polym. Res.* **2020**, *27*, 1–10. [CrossRef]
52. Asefnejad, A.; Khorasani, M.T.; Behnamghader, A.; Farsadzadeh, B.; Bonakdar, S. Manufacturing of biodegradable polyurethane scaffolds based on polycaprolactone using a phase separation method: Physical properties and in vitro assay. *Int. J. Nanomed.* **2011**, *6*, 2375–2384. [CrossRef] [PubMed]
53. Kumar, R.; Kumar, M.; Awasthi, K. Functionalized Pd-decorated and aligned MWCNTs in polycarbonate as a selective membrane for hydrogen separation. *Int. J. Hydrogen Energy* **2016**, *41*, 23057–23066. [CrossRef]
54. Murat, M.; Sorrentino, F. Effect of large additions of Cd, Pb, Cr, Zn, to cement raw meal on the composition and the properties of the clinker and the cement. *Cem. Concr. Res.* **1996**, *26*, 377–385. [CrossRef]
55. Nivethitha, D.; Dharmar, S. Effect of zinc oxide nanoparticle on strength of cement mortar. *IJSTE-Int. J. Sci. Technol. Eng.* **2016**, *3*, 123–127.
56. Barros, A.M.; Espinosa, D.C.R.; Tenório, J.A.S. Effect of Cr_2O_3 and NiO additions on the phase transformations at high temperature in Portland cement. *Cem. Concr. Res.* **2004**, *34*, 1795–1801. [CrossRef]